

Article

Study of Ion Adsorption and Shear Strength of Red Clay under Leaching Action

Yu Song^{1,2}, Hui Li^{1,2}, Yukun Geng^{1,2}, Lulu Xia³ and Rongtao Yan^{1,2,*}¹ School of Civil and Architectural Engineering, Guilin University of Technology, Guilin 541004, China² Guangxi Key Laboratory in Geotechnical Mechanics and Engineering, Guilin 541004, China³ Guangxi Natural Resources Vocational and Technical College, Nanning 531200, China

* Correspondence: 2012019@glut.edu.cn

Abstract: To study the soil-water effect of red clay, a leaching test is conducted by loading red clay into a soil column and collecting the leaching waste liquid periodically for analysis of the ion content and conductivity changes in the leaching waste liquid. After leaching and filtering, the soil is removed from the column and reconstituted as a straight-shear specimen for a straight-shear test. Ca^{2+} , Mg^{2+} , and SO_4^{2-} ions increased and then stabilized in water samples as leaching time increased, while Na^+ , Cl^- , and NO_3^- declined and then stabilized. Due to their presence in the leaching solution, Ca^{2+} , Mg^{2+} , and SO_4^{2-} ions are initially adsorbed by the soil and then saturated by adsorption. In contrast, Na^+ , Cl^- , and NO_3^- precipitate out of the soil due to the dissolution and ion exchange of the soil sample, thereby weakening their effects. Consequently, these ions appear to vary in various ways. The relationship between ion content in solution and conductivity has also been discovered, and the conductivity varies with the total ion charge in the solution. The angle of internal friction decreases as the leaching time increases, but the cohesion of the soil increases.

Keywords: soil and water effects; ion; conductivity; direct shear



Citation: Song, Y.; Li, H.; Geng, Y.; Xia, L.; Yan, R. Study of Ion Adsorption and Shear Strength of Red Clay under Leaching Action. *Sustainability* **2023**, *15*, 959. <https://doi.org/10.3390/su15020959>

Academic Editor: Teodor Rusu

Received: 19 November 2022

Revised: 13 December 2022

Accepted: 15 December 2022

Published: 4 January 2023



Copyright: © 2023 by the authors. Licensee MDPI, Basel, Switzerland. This article is an open access article distributed under the terms and conditions of the Creative Commons Attribution (CC BY) license (<https://creativecommons.org/licenses/by/4.0/>).

1. Introduction

As a regional special soil, red clay has a high water content, a high liquid limit, a high plastic limit, and high porosity ratio [1–3]. It is distributed in most provinces of China, especially in the southwest provinces of Hunan, Guangxi, Guizhou, and Yunnan [4–6]. Red clay is generated through the weathering and lateralization of carbonate rocks, and its formation of red clay varies depending on the region. Red clay from Guilin consists of kaolinite, illite, siderite, alumina trihydrate, potassium feldspar, sodium feldspar, hydro-magnesite, quartz, and other mineral components [7,8]. It is abundant that are hydrophilic, therefore aqueous solutions will affect its properties. When a small amount of water is present in the soil, the soil particles are in direct contact with each other and bond tightly, with the frictional interaction between the particles is dominant. With the increase in water content, the clay minerals in the soil adsorb the bonded water, the bonded water film becomes thinner, the particle spacing decreases, and the water film linking force and the electrostatic gravitational force between the particles increase. When the water content rises again, the water-binding film begins to thicken, free water fills the pores between the particles, the negative charge on the surface of soil particles is largely neutralized by hydrated cations, and the water film linkage and electrostatic gravitational force are significantly weakened.

Guilin is situated in a subtropical monsoon climate zone with an average annual rainfall of 1884 mm [9], and there are more rivers and groundwater. In the presence of aqueous solutions, soils undergo physicochemical changes. This reaction is water-soil action, which modifies the soil properties; Fuller soil and water action as the time of soil and water action increases. [10–19]. Since water usually carries ions in nature, the ions

carried by an aqueous solution are also involved in soil-water action. When specific ions are present in a solution, ion exchange happens, resulting in the transformation of coexisting clay minerals, and the ions in solution are adsorbed by the clay, thus changing the original electrostatic gravitational force [20–24].

Zhang [25] conducted a leaching test on the original red clay of Miaoling. With an increase in leaching time in the Miaoling red clay, the free water in the soil dropped and the bound water increased; the agglomerate structure was destroyed and its structural form changed from a compact grain cluster stacking structure to an aggregate - loose particle structure. Wei [26] discovered that CaSO_4 was soaked by the clay straight shear specimens. Liu [27] measured the electrostatic repulsion in soil water by soaking the soil column with various electrolyte concentration (EC) and sodium adsorption ratio (SAR) solutions. He discovered that the electrostatic repulsion in soil water decreased with increasing electrical conductivity and increased with increasing SAR, and that the decrease of K_s was related to the repulsion in water. Zhang [28] found that the cohesion and internal friction angle of the specimens dropped with soaking time, and the decline of cohesion and internal friction angle reduced with soaking time and finally stabilized by conducting direct shear tests on the red-bedded soft rock at various durations. Wu [29] discovered that the strength of specimens saturated with distilled water was greater than that of specimens saturated with other solutions, and that the cohesive force of specimens saturated in NaCl and AlCl_3 decreased and then increased, while the opposite was true for specimens saturated with CaCl_2 solution. Meng [30] soaked the red clay in NaCl and CaCl_2 solutions, respectively, and discovered that as the solution concentration grew, the plastic limit of the soaked soil samples declined and the liquid limit increased, with the influence of Na^+ ions being stronger than that of Ca^{2+} ions.

Long-term water interaction destabilizes soils composed of red clay. When utilized as a base soil, replacement fill is usually used as a measurement, which inevitably results in waste of resources and environmental damage. However, not all projects require re-filling; therefore, study on the soil and water effects of red clay soils is necessary. In this paper, a leaching test was conducted on Guilin red clay soil using tap water to study the changes in the soil after leaching, and several leaching durations were set for the red clay soil. After leaching, the change of soil shear strength of soil samples with differing leaching durations was evaluated

2. Materials and Methods

The red clay utilized in this experiment was obtained from a depth of around 3 m in the Yanshan District of Guilin, Guangxi. The optimal moisture content was 30%, and the maximum dry density was 1.55 g/cm^3 . The test soil was allowed to naturally dehydrate until its moisture content was stable and easily crushed. The crushed soil is then filtered through a 2 mm sieve and deposited in a bucket for use in the test. In this study, a soil column test was conducted to leach the red clay in the column by loading the red clay into the column and then utilizing the solution to leach the red clay in the column. The peristaltic pump was connected to the solution at one end and the soil column at the other end, and the test solution was pumped to the column at a constant flow rate by the peristaltic pump, the equipment and schematic diagram are shown in Figure 1. This time, tap water was used as the test solution since it is rich in ions and is more similar to the river water, and the test results prove this [31]. According to the pre-experiment, the flow rate of the peristaltic pump was set to 30 mL/min. The experimental periods were set as 1 day, 15 days, 30 days, 45 days, and 60 days, in reference to prior experimental studies [32–34]. At regular intervals, filtered wastewater samples were collected from the outlet of the soil column and the ion concentration and conductivity of the water were measured at each time point. The conductivity of a solution is its ability to conduct an electric current, which can reflect the concentration of ions in the solution, and can also indirectly reflect information such as the salt content and total dissolved solids quality of the solution [35]. It

is a key indicator for detecting the ion-containing, salt-containing, and impurity-containing components of a solution.

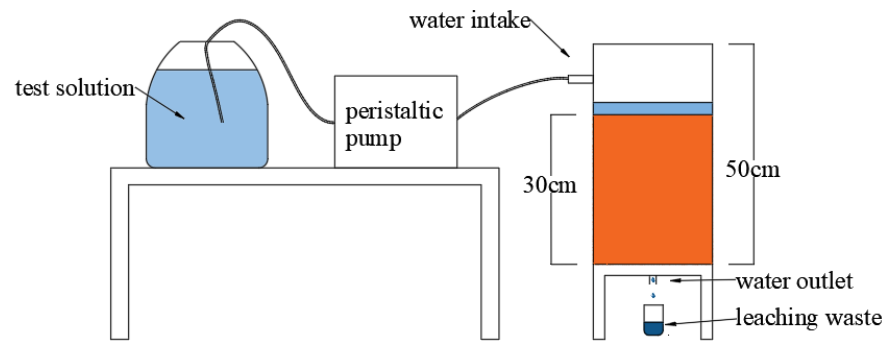


Figure 1. Test setup.

After each group of soil columns had been leached, the test soil was removed from the columns. The soil is air-dried until its moisture content is stable and easily crushed, and then the crushed soil is filtered through a 2mm sieve. According to the 30% moisture content, the water will be sprayed evenly on the soil and thoroughly mixed before being placed in a bag and sealed for several hours to ensure uniform moisture content. In accordance with the geotechnical test specification and previous studies [36–38], the prepared test soil was loaded into the ring knife. Since the roadbed should be more than 90% compacted, the dry density of its straight shear sample is 1.395 g/cm^3 . The ring-knife sample is placed in a vacuum cylinder, sucked and saturated with water for 24 hours. Following that, the straight shear test was started. Five straight shear samples were collected for each leaching time group. The specimens were loaded into the shear box, and each straight shear sample was exposed to 100 kPa, 200 kPa, 300 kPa, 400 kPa, and 500 kPa, respectively, of vertical pressure. After 24 hours of consolidation, the fast shear began. Each specimen group underwent two sets of parallel testing, and the average values were used to obtain the values of cohesion and internal friction angle using the Coulomb formula. The formula is as follows:

$$\tau_f = c + \sigma \tan \varnothing \quad (1)$$

τ_f is the shear strength; c is the cohesion of the soil, σ is the total stress; \varnothing is the angle of internal friction of the soil.

3. Experimental Results and Discussion

3.1. Analysis of Ion Change in Water Sample

Figure 2 depicts the ion concentration of the dewatering waste solution and the ion concentration of the test solution at various leaching times. The Ca^{2+} , Mg^{2+} , and SO_4^{2-} concentration in the water were low at the beginning of the experiment, as shown by the graph, but began to rise as leaching time increased. The concentrations of Na^+ , Cl^- , and NO_3^- in the water dropped as leaching time increased. In contrast, Al^{3+} , K^+ , and F^- did not change appreciably.

As indicated in Figure 3, the Ca^{2+} concentration ranges between 1.498 and 15.68 mg/L, the Mg^{2+} concentration ranges between 0.165 and 1.063 mg/L, and the SO_4^{2-} concentration ranges between 0.902 and 3.476 mg/L. Since the variations in Ca^{2+} were comparable to those of Mg^{2+} and SO_4^{2-} , but the changes of the Ca^{2+} interval were greater, Ca^{2+} was used as the primary object of analysis. Initially, the Ca^{2+} ion concentration in the water sample was low and significantly lower than the Ca^{2+} ion concentration in the test solution. This is due to the fact that Ca^{2+} in the aqueous solution was adsorbed by the soil, resulting in a reduction in Ca^{2+} concentration in the aqueous solution. At the beginning of the test, the quantity of ions adsorbed in the soil particles was low and it had a relatively large adsorption capacity, and the Ca^{2+} concentration in the test solution was high, so more Ca^{2+} could be adsorbed; additionally, the majority of the soil had a preference for Ca^{2+}

adsorption and was more likely to adsorb Ca^{2+} [39]. As the drenching time increased, Ca^{2+} in the drenching waste stream grew as a result of a rise in Ca^{2+} adsorption in the soil, and the soil's adsorption capacity for Ca^{2+} began to weaken, leading to an increase in Ca^{2+} in the water sample. In the later stage, Ca^{2+} in the leachate almost stabilized and did not change much.

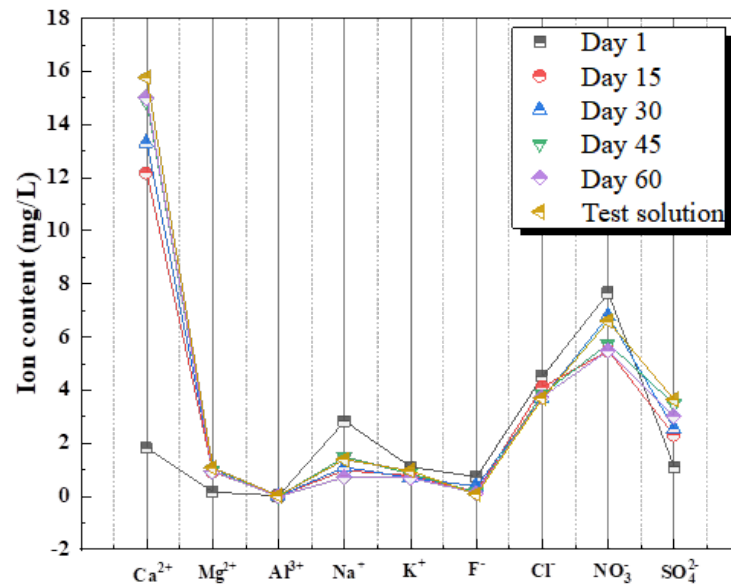


Figure 2. Variation of ion content with leaching time.

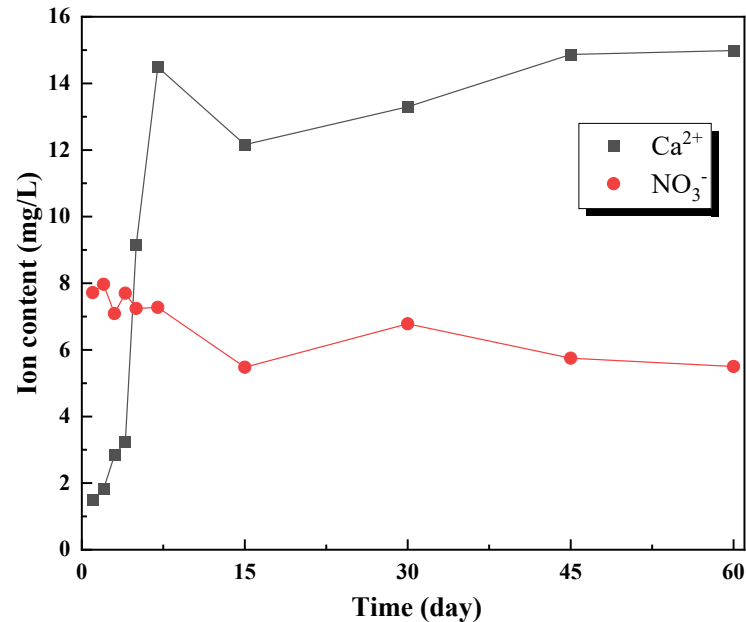


Figure 3. Ca^{2+} and, NO_3^- ionic content change diagram.

The change in Na^+ concentration ranged from 0.979 to 2.83575 mg/L. With increasing leaching time, the Na^+ concentration in the water sample began to decline and eventually stabilized at approximately 1 mg/L. This may be because the clay with adsorbed Na^+ ions initially encountered free Ca^{2+} ions or other cations, releasing the Na^+ ions and adsorbed the Ca^{2+} ions for cation exchange. Consequently, the water sample contains more Na^+ ions and less Ca^{2+} ions than the initial solution. After a period of leaching, the adsorption and desorption of Na^+ ions by the clay are in dynamic equilibrium, thus the

Na⁺ ion concentration in the later water samples is approximately 1 mg/L, which is comparable to the ion concentration of the solution (Figure 4).

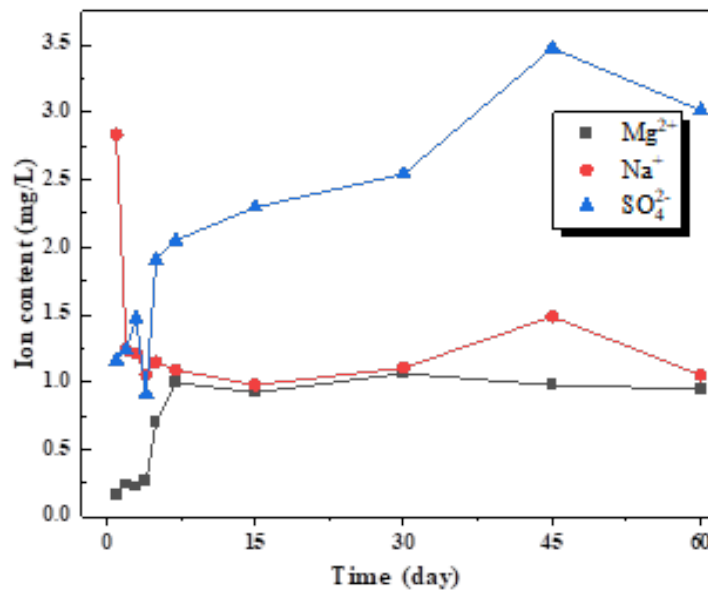


Figure 4. Mg²⁺, Na⁺, SO₄²⁻ ionic content change diagram.

Cation exchange processes have a crucial function in controlling the chemical composition of groundwater [40]. The soil retains cations by electrostatic action, and the initial cations are easily exchanged with other cations in solution due to electrostatic action [41]. Its cation exchange follows a specific pattern [42,43]. Because Ca²⁺ ion exchange capacity is greater than that of Na⁺, it is easy to adsorb on the surface of soil particles and replace the Na⁺ adsorbed on the surface of soil particles again, balancing part of the negative charge; its cation exchange principle is depicted in Figure 5; therefore, Ca²⁺ and Na⁺ in the leaching waste solution appear in various forms. The fluctuations of Mg²⁺ and the underlying causes were similar to those of Ca²⁺, but the Mg²⁺ concentration in the test solution was lower, therefore it rapidly stabilized. In the early stage of the test, the NO₃⁻ concentration in the leachate was greater than the NO₃⁻ concentration in the test solution, and then gradually decreased and finally stabilized. This may be the result of the competing adsorption of NO₃⁻ and SO₄²⁻, with SO₄²⁻ displacing NO₃⁻. Similar trends are observed for SO₄²⁻ and Ca²⁺ due to the cation induced adsorption of SO₄²⁻ to balance its charge. Thus, the adsorption of Ca ions by the soil increased and that of SO₄²⁻ also increased [44,45].

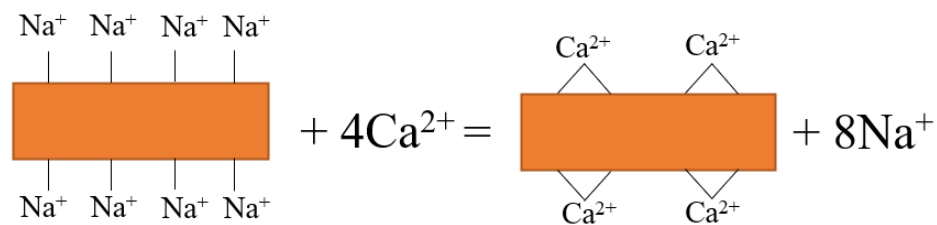


Figure 5. Principle of ion exchange reaction.

3.2. Analysis of Conductivity Changes in Water Samples

When a solution is more pure, its conductivity is diminished and its conductivity is reduced. It can be seen in Figure 6a that the conductivity first declines with time before rising and then stabilizing. Since the conductivity values are impacted by temperature, ion species, and ion concentration [46,47], the conductivity variation in this test is primarily attributable to the change in different ion concentration. Since the total ion change does not correspond with the conductivity change, the valence of the ions was taken into account.

To examine the relationship between the valence number and concentration of ions in their solutions relate to the change in conductivity. The ion concentration was transformed to electrons using the following equation.

$$n_i = \frac{m_i}{M_i} \quad (2)$$

$$e_i = n_i * E_i \quad (3)$$

$$e = \sum e_i \quad (4)$$

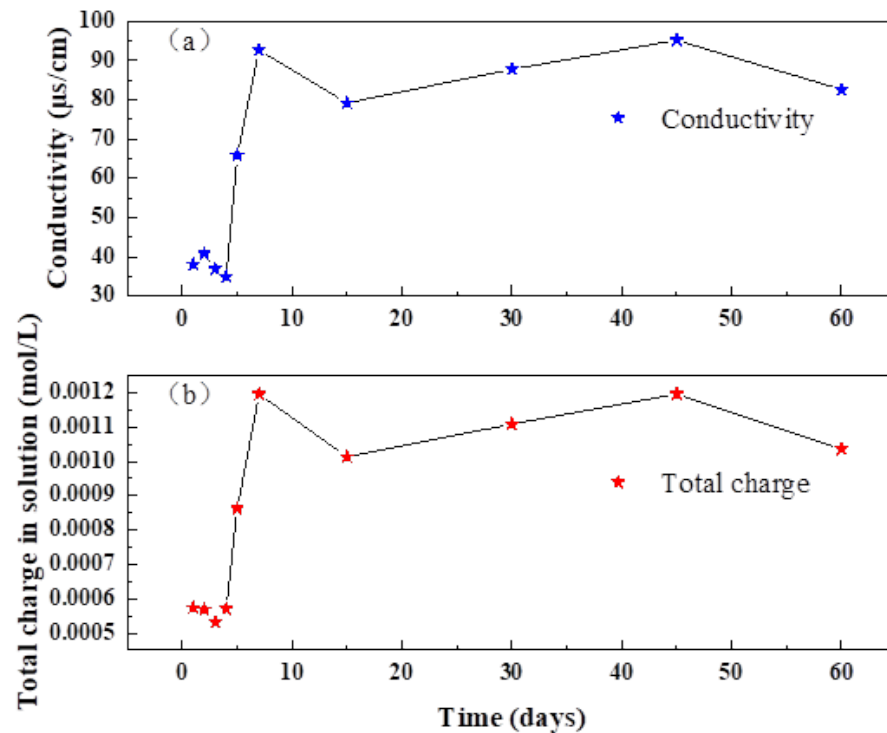


Figure 6. Conductivity and total charge in solution as a function of time. (a) Electrical conductivity in solution as a function of time (b) Total charge in solution as a function of time.

The formula n_i is the molar concentration of an ion (mol/L), m_i is the mass concentration of an ion (g/L), M is the relative atomic mass, e_i is the total number of electrons lost or gained by an ion in the solution, and E_i is the number of electrons lost or gained by an ion. e is the total number of electrons lost or gained by all ions in the solution.

The mass concentration of ions in the solution was calculated to obtain the sum of all positive and negative electron numbers, and the resulting total charge per liter of the solution was compared with the conductivity, as depicted in Figure 5. This comparison reveals that both the conductivity and the total charge decreased initially and then increased with time, exhibiting similar trends. Figure 7 depicts a one-dimensional linear fit of the conductivity to the total amount of charges, with the fitting equation being

$$\sigma = 90083.26425e - 12.60317 \quad (5)$$

where, σ is the electrical conductivity ($\mu\text{S}/\text{cm}$)

The fit is displayed in the table below, and its fitted result R-squared is 0.993, indicating that the fit equation is a good match and that the two data sets are linear. The range of its Durbin-Watson value is 0–4, and the data are independent. f is 1314.931, $p < 0.001$. Consequently, the model effectively depicts the relationship between conductivity and ionic concentration (Table 1).

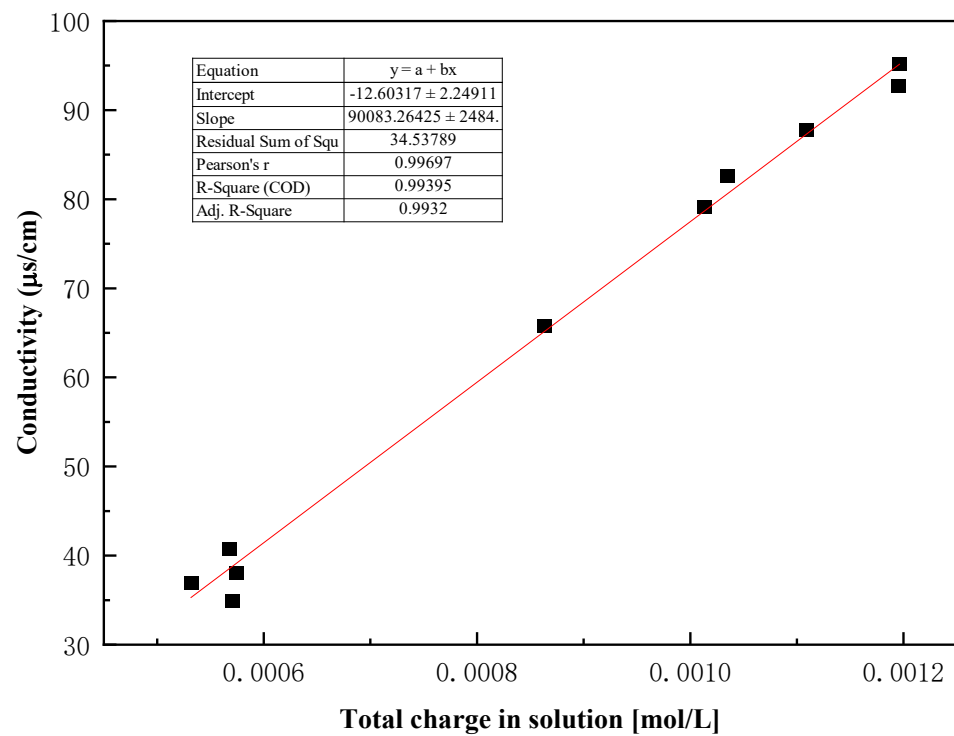


Figure 7. Model of ion concentration and conductivity.

Table 1. Model parameters.

R	R-Squared	Adjusted R-Square	Durbin-Watson	F
0.997	0.994	0.993	2.461	1314.931

The above equations were integrated to establish a mathematical model between solution ion concentration and solution conductivity, and the equation is shown below:

$$\sigma = 90083.26425 \sum \frac{m_i}{M_i} E_i - 12.60317 \quad (6)$$

When temperature and ion species are held constant, the change in solution conductivity is primarily caused by the change in the concentration of each ion in the solution; and the higher the valence of the ion, the more pronounced the effect of the change in its ion concentration on the solution conductivity. As the ion concentration rises, so does the solution conductivity.

3.3. Analysis of the Variation of Strength Index of Soil Samples

Figure 8 depicts the variations in cohesion and internal friction angle of the soil samples after different times of leaching. The cohesive force of soil samples grew steadily as leaching time increased. And the cohesion diminished as the leaching time increased. Red clay cohesion depends on the gravitational force of soil particles, the water film force, and the cementing force generated by the cementing material in the soil. According to studies, soils containing montmorillonite, kaolinite, and illite are susceptible to the influence of Mg ions [48]. Mg influences the structural stability of the soil [49], resulting in a greater swelling of the clay due to its greater hydration energy and wider hydration shell. Greater swelling inevitably results in weakened aggregate bonds, which diminishes the stability of the soil sample. Since the solution contains Mg^{2+} , which is adsorbed by the soil sample, there is a moderate increase in soil cohesion after a brief soaking. The adsorption of Ca^{2+} increased in consecutive soil samples, while the adsorption of Mg^{2+} remained stable. The Ca^{2+} ions adsorbed in the soil sample played a calcium cementation role, the soil

particles were cathodic, the Ca^{2+} ions in the solution exchanged with K^+ and Na^+ ions on the clay surface, and the negative soil particles directly adsorbed the Ca^{2+} ions in the solution; after ion exchange and the adsorption of calcium ions on the soil particles, the film water on the surface of the soil particles became thinner, the molecular attraction between the soil particles increased, and the strength of the soil was improved. The closer the structure between soil particles, the more cohesive its force. The internal friction is a function of the particle size, roughness, and compactness of the soil body. After prolonged water leaching, the particle size and structure of the soil body are altered, and the test soil sample becomes more rounded and smoother, so the internal friction angle decreases as leaching time increases. Consequently, the cohesion and the angle of internal friction of the soil samples after leaching exhibit such a change pattern

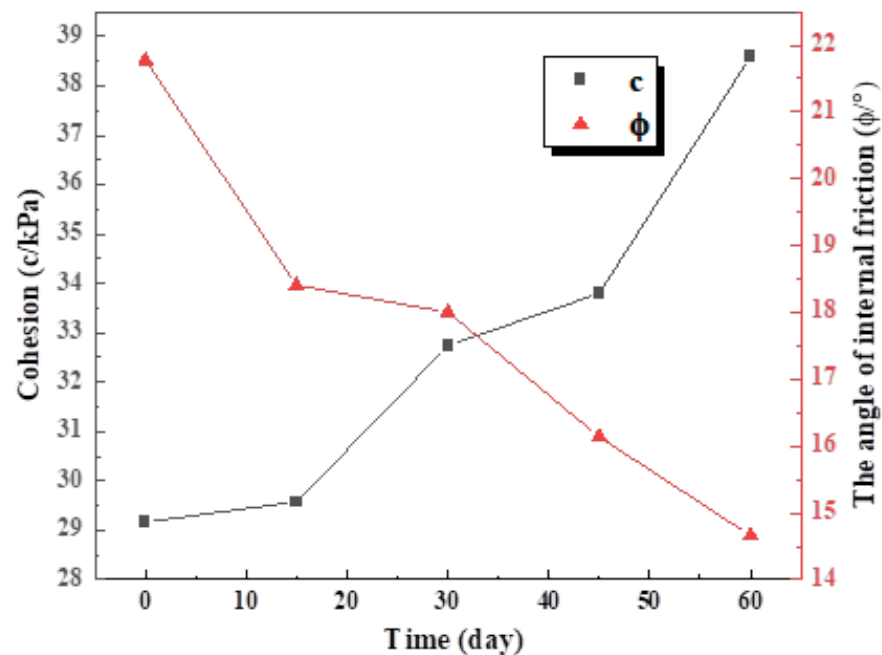


Figure 8. Variation of cohesion and internal friction angle of soil samples with different leaching times.

4. Conclusions

We conducted a leaching test on the red clay to study the ion changes and conductivity changes in the leaching waste solution, and a direct shear test on the leached soil to study the changes in the cohesion and internal friction angle of the specimens, and found the following:

1. With the increase of leaching time, the Ca^{2+} , Mg^{2+} , and SO_4^{2-} ions in the water samples increased and then decreased because the soil adsorbed these ions in the solution at the beginning, resulting in the decrease of ion content in the water samples. The ion content of Na^+ , Cl^- , and NO_3^- ions decreases and then stabilizes because the ion content in the water sample increases due to the decomposition and precipitation of these ions in the soil as a result of leaching.
2. The content of each ion in the water sample was converted into the total charge carried by the ions and fitted with the conductivity model, which was found to be a good response to the changes in conductivity, indicating that the change in the total amount of ions in the water sample is the main factor affecting the conductivity, and the solution ions can be judged indirectly through the conductivity.
3. Soil samples with different leaching times were made into remodeled straight shear samples. It was found that the cohesion of the soil samples gradually increased because the molecular attraction between the soil particles increased after the adsorption of calcium ions by the leaching effect, and the strength of the soil was improved, and the structure between the soil particles was tightened. The cohesive force is increased.

The internal friction angle decreases with the increase of leaching time, because the soil particles become rounded and smooth by leaching, thus reducing the internal friction angle.

Author Contributions: Conceptualization, Y.S.; validation, Y.G., L.X.; data curation, L.X., H.L.; writing—original draft preparation, H.L.; writing—review and editing, R.Y.; supervision, Y.S.; project administration, R.Y.; All authors have read and agreed to the published version of the manuscript.

Funding: 1. Guangxi Innovation-Driven Development Special Project (Guik AA20161004-1). 2. National Key Research and Development Program Project (2019YFC0507502). 3. National Natural Science Foundation of China (41967037). 4. National Natural Science Foundation of China (42262030).

Institutional Review Board Statement: Not applicable.

Informed Consent Statement: Not applicable.

Conflicts of Interest: The authors declare no conflict of interest.

References

- Xiao, G.Y.; Ye, Z.M.; Xu, G.L.; Zeng, J.; Zhang, L. Temperature Effect on Crack Evolution of Red Clay in Guilin. *Water* **2021**, *13*, 3025. [[CrossRef](#)]
- Lei, W. Study on Dynamic Characteristics of Phosphogypsum Stabilized Soil Subgrade. Master's Thesis, Guizhou University, Guiyang, China, 2021.
- Li, S.M.; Wu, M.; Meng, J.P.; Liu, Z.K. Influence of compactness and initial moisture content on disintegration characteristics of red clay. *J. Henan Univ. Sci. Technol.* **2021**, *42*, 54–59.
- Chen, X.J.; Qi, Y.L.; Lu, L.X.; Liu, X.M.; Xiao, G.Y. Impact of Different Preparation Methods on the Optimum Moisture Content and Maximum Dry Density of Guilin Red Clay. *Saf. Environ. Eng.* **2013**, *20*, 136–139.
- Weng, Z.Y.; Wang, L.N.; Liu, Q.; Pan, X.M.; Xu, Y.H.; Li, J. Improving the unconfined compressive strength of red clay by combining biopolymers with fibers. *J. Renew. Mater.* **2021**, *9*, 1503–1517. [[CrossRef](#)]
- D'Angelo, B.; Bruand, A.; Qin, J.T.; Peng, X.H.; Hartmann, C.; Bo, S.; Hao, H.T.; Rozenbaum, O.; Muller, F. Origin of the high sensitivity of Chinese red clay soils to drought: Significance of the clay characteristics. *Geoderma* **2014**, *223*, 46–53. [[CrossRef](#)]
- Lv, H.B.; Zeng, Z.T.; Yin, G.Q.; Zhao, Y.L. Analysis of mineral composition of red clay in Guangxi. *J. Eng. Geol.* **2012**, *20*, 651–656.
- Xu, Y.S. Study on Thermal Properties of Lateritic Clay and Its Influence on Heat Transfer Performance of Vertical Buried Pipe in Karst Area. Doctoral Dissertation, Shanghai University, Shanghai, China, 2020.
- Zhang, Y. Guilin Construction of Sponge City: Wisdom between Tonna. *Guilin Dly.* **2022**. [[CrossRef](#)]
- Wen, B.P.; He, L. Influence of lixiviation by irrigation water on residual shear strength of weathered red mudstone in Northwest China: Implication for its role in landslides' reactivation. *Eng. Geol.* **2012**, *151*, 56–63. [[CrossRef](#)]
- Turkoz, M.; Savas, H.; Acaz, A.; Tosin, H. The effect of magnesium chloride solution on the engineering properties of clay soil with expansive and dispersive characteristics. *Appl. Clay Sci.* **2014**, *101*, 1–9. [[CrossRef](#)]
- Al Hattamleh, O.; Aldeeky, H.; Rabab'ah, S.; Taamneh, M. The effect of Dead Sea salt solution on the engineering properties of expansive subgrade clayey soil. *Arab. J. Geosci.* **2020**, *13*, 1–11. [[CrossRef](#)]
- Yan, R. BBM-Type constitutive model for coupled chemomechanical behavior of saturated soils. *Int. J. Geomech.* **2018**, *18*, 06018023. [[CrossRef](#)]
- Yan, R.T.; Zhang, Q. A constitutive model of expansive clay considering thermos-hydro-mechanical coupling effect. *Environ. Earth Sci.* **2019**, *78*, 277. [[CrossRef](#)]
- Zeng, Z.T.; Pan, B.; Wu, Y.D.; Zhang, B.H.; Liang, Z. Influence Mechanism of Bound Water on Shear Strength Characteristics of Lateritic. *Chin. J. Undergr. Space Eng.* **2022**, *18*, 1565–1572+1579.
- Wu, Y.D. Research on Influence of Water Content on Physical-Mechanical Properties of Red Clay and Its Micro-Mechanism. Master's Thesis, Guilin University of Technology, Guilin, China, 2019.
- Hong, W.T.; Jung, Y.S.; Kang, S.; Lee, J.S. Estimation of soil-water characteristic curves in multiple-cycles using membrane and TDR system. *Materials* **2016**, *9*, 1019. [[CrossRef](#)]
- Ding, L.; Zhang, J.; Deng, Z. Effect of bound water on mechanical properties of typical subgrade soils in southern China. *Geomech. Eng.* **2021**, *27*, 573–582.
- Yao, Y.S.; Li, J.; Xiao, Z.Q.; Xiao, H.B. Soil-Water characteristics and creep deformation of unsaturated expansive subgrade soil: Experimental test and simulation. *Front. Earth Sci.* **2021**, *9*, 783273. [[CrossRef](#)]
- Zhang, F.Y.; Wang, G.H.; Kamai, T.; Chen, W.W.; Zhang, J.Y. Undrained shear behavior of loess saturated with different concentrations of sodium chloride solution. *Eng. Geol.* **2013**, *155*, 69–79. [[CrossRef](#)]
- Tiwari, B.; Ajmera, B. Reduction in fully softened shear strength of natural clays with NaCl leaching and its effect on slope stability. *J. Geotech. Geoenvironmental Eng.* **2015**, *141*, 04014086. [[CrossRef](#)]
- Feng, S.J.; Chen, Z.W.; Chen, H.X.; Zheng, Q.T.; Liu, R. Slope stability of landfills considering leachate recirculation using vertical wells. *Eng. Geol.* **2018**, *241*, 76–85. [[CrossRef](#)]

23. Fu, J.T.; Hu, X.S.; Li, X.L.; Yu, D.M.; Liu, Y.B.; Yang, Y.Q.; Qi, Z.X.; Li, S.X. Influences of soil moisture and salt content on loess shear strength in the Xining Basin, northeastern Qinghai-Tibet Plateau. *J. Mt. Sci.* **2019**, *16*, 1184–1197. [[CrossRef](#)]
24. Chen, B.; Peng, F.; Zhang, L.; Sun, D.A. Investigation on swelling characteristics of GMZ bentonite with different initial water contents. *Ann. Nucl. Energy* **2023**, *181*, 109565. [[CrossRef](#)]
25. Zhang, W.B.; Bai, W.; Kong, L.W.; Fan, H.H.; Yue, X. Effect of leaching time on physical and mechanical characteristics of lateritic soil. *Rock Soil Mech.* **2022**, *43*, 443–452.
26. Wei, T.; Chen, G.Q.; Sun, X.; Li, Y.; Qin, C.G.; Yan, M. Shear strength and microstructure of silty clay subjected to CaSO₄ solution and stability effect on a gypsum dump. *Bull. Eng. Geol. Environ.* **2021**, *80*, 4143–4157. [[CrossRef](#)]
27. Liu, X.M.; Zhu, Y.C.; Bennett, J.M.; Wu, L.S.; Li, H. Effects of sodium adsorption ratio and electrolyte concentration on soil saturated hydraulic conductivity. *Geoderma* **2022**, *414*, 115772. [[CrossRef](#)]
28. Zhang, S.; Xu, Q.; Hu, Z.M. Effects of rainwater softening on red mudstone of deep-seated landslide, Southwest China. *Eng. Geol.* **2016**, *204*, 1–13. [[CrossRef](#)]
29. Wu, M.; Li, S.M. The microscopic mechanism of mohr-coulomb strength theory of saturated lateritic soil. In Proceedings of the 2021 Industrial Architecture Academic Exchange Conference, Beijing, China, 9 November 2021; p. 6.
30. Meng, G.L.; Chen, Y.F.; Wang, G.W.; Liu, Z.K. Study on the Effect of Water-soil Interaction on the Engineering Property of Remodeling Red Clay in Guilin. *Sci. Technol. Eng.* **2017**, *17*, 265–271.
31. Liu, J.W. Experimental Study on Soil Micro—Structure and Shear Strength under the Action of Hydration Effects. Master’s Thesis, China University of Geosciences, Wuhan, China, 2012.
32. Wang, W.Y.; Li, R.B.; Tan, J.A.; Luo, K.L.; Yang, L.S.; Li, Y.H. Adsorption and leaching of fluoride in soils of China. *Fluoride* **2002**, *35*, 122–129.
33. Leiva, C.; Ahumada, I.; Sepúlveda, B.; Richter, P. Polychlorinated biphenyl behavior in soils amended with biosolids. *Chemosphere* **2010**, *79*, 273–277. [[CrossRef](#)]
34. Kang, X.; Wang, S.; Yu, Z. Effects of Soil–Water Interaction on the Mechanical Behaviors of Shear-Zone Soils. *Int. J. Geomech.* **2022**, *22*, 06022028. [[CrossRef](#)]
35. Yu, X. The Detection Technology and Experimental Research of a New Type of Electrical Conductivity and pH of Water Quality Parameters. Master’s Thesis, Zhejiang University, Hangzhou, China, 2015.
36. Hyodo, T.; Wu, Y.; Hyodo, M. Influence of fines on the monotonic and cyclic shear behaviour of volcanic soil “Shirasu”. *Eng. Geol.* **2022**, *301*, 106591. [[CrossRef](#)]
37. Wu, Y.; Cui, J.; Huang, J.; Zhang, W.; Yoshimoto, N.; Wen, L. Correlation of critical state strength properties with particle shape and surface fractal dimension of clinker ash. *Int. J. Geomech. ASCE* **2021**, *21*, 04021071. [[CrossRef](#)]
38. Bing, H.; Zhang, Y.; Ma, M. Impact of Desalination on Physical and Mechanical Properties of Lanzhou Loess. *Eurasian Soil Sci.* **2017**, *50*, 1444–1449. [[CrossRef](#)]
39. Rahman, W.A.; Rowell, D.L. The influence of magnesium in saline and sodic soils; a specific effect or a problem of cation exchange? *J. Soil Sci.* **1979**, *30*, 535–546. [[CrossRef](#)]
40. Jankowski, J.; Acworth, R.I. Impact of debris-flow deposits on hydrogeochemical processes and the development of dryland salinity in the Yass River Catchment, New South Wales. *Australia. Hydrogeol. J.* **1997**, *5*, 71–88. [[CrossRef](#)]
41. Dawid, J.; Dorota, K. A comparison of methods for the determination of cation exchange capacity of soils. *Ecol. Chem. Eng.* **2014**, *21*, 487–498.
42. Guo, A.; Ke, Z.H.; Qiu, X.Y.; Lan, Q.F.; Xiao, L. Study on green and ammonium-free leaching agent for ion-absorbed rare earth ore. *China Nonferrous Metall.* **2022**, *51*, 79–85.
43. Sheng, W.K. The Influence of Seawater Intrusion to Heavy Metal Elements in Soil—A Case Study of Pearl River Delta, China. Master’s Thesis, China University of Geosciences, Beijing, China, 2020.
44. Zhou, W.; Lin, B. Advances in the study of sulfur behavior in soils and plants. *Soils Fertil.* **1997**, *5*, 8–11.
45. Bolan, N.S.; Syers, J.K.; Sumner, M.E. Calcium-induced sulfate adsorption by soils. *Soil Sci. Soc. Am. J.* **1993**, *57*, 691–696. [[CrossRef](#)]
46. Qi, Y.; Lu, Y.; Zhou, Q.Q.; Kan, Z.T.; Yang, L.; Bai, X.; Dong, B.; Xu, L. Application of High Performance Hydrogels in Wearable Sensors. *Chin. J. Anal. Chem.* **2022**, *50*, 1699–1711.
47. Gao, P. Spatial Multi-Scale Variation, Driving Mechanism, Prediction and Early Warning of Soil Salinization in the Coastal Area of the Yellow River Delta. Doctoral Dissertation, Shandong Agricultural University, Taian, China, 2022.
48. Zhang, X.C.; Norton, L.D. Effect of exchangeable Mg on saturated hydraulic conductivity, disaggregation and clay dispersion of disturbed soils. *J. Hydrol.* **2002**, *260*, 194–205. [[CrossRef](#)]
49. Curtin, D.; Steppuhn, H.; Selles, F. Effects of magnesium on cation selectivity and structural stability of sodic soils. *Soil Sci. Soc. Am. J.* **1994**, *58*, 730–737. [[CrossRef](#)]

Disclaimer/Publisher’s Note: The statements, opinions and data contained in all publications are solely those of the individual author(s) and contributor(s) and not of MDPI and/or the editor(s). MDPI and/or the editor(s) disclaim responsibility for any injury to people or property resulting from any ideas, methods, instructions or products referred to in the content.